

## Searching for Isolated Black Hole Candidates within 15 pc of the Solar System in Gaia DR3

ABDURAKHMON NOSIROV ,<sup>1,2</sup> COSIMO BAMBI ,<sup>1,3,\*</sup> LEDA GAO ,<sup>1</sup> JOS DE BRUIJNE ,<sup>4</sup> JIACHEN JIANG ,<sup>5</sup>  
 ANDREA SANTANGELO ,<sup>2,1</sup> AND FU-GUO XIE ,<sup>6</sup>

<sup>1</sup>Center for Astronomy and Astrophysics, Department of Physics, Fudan University, Shanghai 200438, China

<sup>2</sup>Institut für Astronomie und Astrophysik, Eberhard-Karls Universität Tübingen, D-72076 Tübingen, Germany

<sup>3</sup>School of Humanities and Natural Sciences, New Uzbekistan University, Tashkent 100001, Uzbekistan

<sup>4</sup>Directorate of Science, European Space Research and Technology Centre, NL-2201 AZ Noordwijk, The Netherlands

<sup>5</sup>Department of Physics, University of Warwick, Coventry CV4 7AL, UK

<sup>6</sup>Shanghai Astronomical Observatory, Chinese Academy of Sciences, Shanghai 200030, China

### ABSTRACT

Theoretical models predict that the Galaxy hosts  $10^8$ - $10^9$  black holes formed from the complete gravitational collapse of heavy stars and that most of these black holes are isolated, without any companion. Within 15 pc of the Solar System ( $\sim 50$  ly), there may be a few black holes. If located inside one of the Local Interstellar Clouds – which occupy 5-20% of this local volume – an isolated black hole could produce detectable electromagnetic emission via accretion from the interstellar medium, given the capabilities of current or near-future observatories. However, precise predictions remain challenging due to large uncertainties in the expected accretion spectra. Outside these clouds, the accretion rate would be too low in any standard model to yield a detectable electromagnetic signal. While astrometric detection via gravitational perturbation of nearby stars is conceivable, the local stellar density is too low for this method to be realistically successful. We have searched the Gaia DR3 catalog for candidate isolated black holes accreting from the interstellar medium and identified five sources. All candidates lie close to the Galactic plane, making them likely spurious astrometric solutions, for instance caused by unmodelled background sources (crowding) and/or unmodelled binarity; nevertheless, they cannot be definitively ruled out without follow-up observations.

### 1. INTRODUCTION

Black holes represent one of the most intriguing predictions of Einstein’s theory of General Relativity and serve as ideal laboratories for testing gravity in the strong-field regime (Bambi 2017a,b; Yagi & Stein 2016; Bambi & Cárdenas-Avendaño 2024). Prior to 2015, their observational evidence was indirect, relying on inferences from stellar-mass black holes in X-ray binaries and supermassive black holes in galactic nuclei. The identification of these objects as the Kerr black holes of General Relativity (Kerr 1963; Carter 1971; Robinson 1975) was largely due to the absence of alternative explanations within conventional physics: stellar-mass black holes exceeded the maximum theoretical mass of neutron stars (Rhoades & Ruffini 1974; Lattimer 2012), while supermassive black holes were too massive, compact, and old to be clusters of neutron stars (Maoz 1998). Today, we can directly probe the nature of these objects through gravitational waves (e.g., Abbott et al.

2016, 2019), X-ray observations (e.g., Cao et al. 2018; Tripathi et al. 2019a,b, 2021), and black hole imaging (e.g., Psaltis et al. 2020; Vagozzi et al. 2023), confirming the predictions of General Relativity within the precision of our measurements.

While the next generation of observational facilities will improve existing constraints, performing very precise and accurate tests of General Relativity with astrophysical observations may remain difficult due to the complex astrophysical environments around black holes. This motivates consideration of alternative approaches, such as sending a probe to orbit a nearby black hole (Bambi 2025a,b). Although extremely challenging, such a mission – employing a small spacecraft or fleet of small spacecraft – is not inconceivable in the coming decades. A critical requirement is that the target black hole lie within 15 pc (approximately 50 ly) of the Solar System; at greater distances, a complete mission profile – including travel, operations, and data return – would exceed a century even for a spacecraft traveling near the speed of light.

\* bambi@fudan.edu.cn

Motivated by this visionary idea, in this work we investigate the possibility of discovering an isolated black hole within 15 pc of the Solar System. As first noted by [Shvartsman \(1971\)](#), an isolated black hole can accrete from the interstellar medium, potentially producing detectable electromagnetic radiation. Subsequent studies have explored this topic ([Meszaros 1975](#); [McDowell 1985](#); [Fujita et al. 1998](#); [Maccarone 2005](#); [Fender et al. 2013](#); [Tsuna et al. 2018](#); [Scarella et al. 2021](#); [Murchikova & Sahu 2025](#)), though most have focused on isolated black holes in relatively high-density environments rather than on nearby objects.

Within 15 pc of the Solar System, 80-95% of the volume is filled with a hot, low-density interstellar medium ([Redfield & Linsky 2008](#)). As shown in the following section, the particle density in this region is too low for accretion onto an isolated black hole to produce a luminosity above the detection threshold of current or near-future facilities, regardless of the accretion model. The situation changes if a black hole resides within one of the Local Interstellar Clouds, where the interstellar medium is warm, partially ionized, and denser. These clouds occupy only 5-20% of the local volume, reducing the probability of finding a black hole inside them. Nevertheless, as discussed in subsequent sections, there are reasonable prospects for detecting such objects – should they exist – in the near future, despite large uncertainties in their expected accretion spectra.

We therefore search the Gaia DR3 catalog for candidate isolated black holes accreting from the interstellar medium and identify five sources. All lie close to the Galactic plane, making them likely spurious astrometric solutions; however, they cannot be ruled out as genuine black holes without further observations. We also consider the possibility of indirectly detecting non-accreting isolated black holes through their gravitational influence on the motions of nearby stars. However, the low stellar density in the Solar neighborhood makes close encounters between a black hole and a star extremely unlikely on human timescales.

This manuscript is organized as follows. In Section 2, we review estimates of the black hole population within 15 pc of the Solar System. In Section 3, we discuss accretion from the interstellar medium onto an isolated black hole and compare predicted spectra with detection thresholds of current catalogs. Our search for candidates in Gaia DR3 is presented in Section 4. A summary and our conclusions are given in Section 5.

## 2. POPULATION OF NEARBY BLACK HOLES

Estimates of the population of black holes in the Solar neighborhood are subject to significant uncertainties,

encompassing their number, local environments, and expected spectra. In this section, we review and elaborate on previous estimates of the expected abundance of black holes within 15 pc of the Solar System. We conclude that it is plausible for a few such objects to reside within this volume.

Theoretical models suggest the Galaxy contains between  $\sim 10^8$  ([Olejak et al. 2020](#)) and  $\sim 10^9$  ([Timmes et al. 1996](#)) stellar-mass black holes ( $N_{\text{BH}}$ ). Most are expected to be isolated, having lost any companion star during their evolution. Although most massive stars form in binary systems, the binary survival probability is low: systems with small separations may merge during the red supergiant phase of the massive star, while wider systems are typically disrupted by the supernova explosion that produces the black hole. [Olejak et al. \(2020\)](#) estimate that the Galactic disk hosts  $\sim 1.0 \cdot 10^8$  isolated black holes and  $\sim 8 \cdot 10^6$  black holes in binary systems; of the latter, about 80% have another black hole as a companion, and fewer than 2% are paired with a normal star.

To estimate the proximity of the nearest black hole, we consider two approaches. [Fender et al. \(2013\)](#) model the Galaxy as a disk (radius 10 kpc, thickness 0.5 kpc) plus a bulge (radius 2 kpc), yielding a total volume  $V_{\text{Gal}} \sim 200 \text{ kpc}^3$ . The average volume per black hole is therefore  $V_{\text{BH}} = V_{\text{Gal}}/N_{\text{BH}}$ , ranging from  $200 \text{ pc}^3$  (for  $N_{\text{BH}} = 10^9$ ) to  $2,000 \text{ pc}^3$  (for  $N_{\text{BH}} = 10^8$ ). If we model this volume as a sphere, its radius ranges from 3.6 pc to 7.8 pc, respectively. Placing the Solar System at the center of such a sphere implies the nearest black hole lies within 3.6-7.8 pc, with an expected distance in the range 2.9-6.2 pc (9.5-20 ly).

[Murchikova & Sahu \(2025\)](#) adopt a different method, based on the total stellar mass of the Galaxy,  $M_{\text{star}} = (6.1 \pm 1.1) \cdot 10^{10} M_{\odot}$ . The ratio  $M_{\text{star}}/N_{\text{BH}}$  then ranges from  $\sim 60 M_{\odot}$  (for  $N_{\text{BH}} = 10^9$ ) to  $\sim 600 M_{\odot}$  (for  $N_{\text{BH}} = 10^8$ ). With a local stellar mass density  $\rho_{\text{star}} \sim 0.04 M_{\odot} \text{ pc}^{-3}$  ([Lutsenko et al. 2025](#)), the average volume per black hole near the Sun is  $V_{\text{BH}} = (M_{\text{star}}/N_{\text{BH}})/\rho_{\text{star}}$ , or 1,500-15,000 pc $^3$ . Modeling this as a sphere gives a radius of 7-15 pc. The expected distance to the nearest black hole would thus be 5.6 pc (18 ly) if within 7 pc, or 12 pc (40 ly) if within 15 pc.

Combining these estimates, the nearest black hole may lie at  $\sim 10$ -20 ly (from [Fender et al. 2013](#)) or  $\sim 20$ -40 ly (from [Murchikova & Sahu 2025](#)). However, the latter approach may overestimate the distance, as the local stellar mass density  $\rho_{\text{star}}$  does not account for remnant mass (e.g., neutron stars and black holes) or ejected material. Since the Solar neighborhood lacks very young stars, the original massive stars have already evolved,

leaving a lower present-day  $\rho_{\text{star}}$  than in star-forming regions, potentially biasing the inferred black hole distance upward.

The location of the Solar System within a spiral arm further influences these estimates. Although the mass density in spiral arms is only  $\sim 20\text{-}30\%$  higher than in inter-arm regions, massive star formation – and thus black hole production – is significantly enhanced there. This is evidenced by the concentration of black hole low-mass X-ray binaries in spiral arms (e.g., [Abdulghani et al. 2025](#)). If we assume black holes are confined to spiral arms (which occupy  $\sim 20\%$  of the Galactic disk volume), the effective volume  $V_{\text{Gal}}$  in the model of [Fender et al. \(2013\)](#) reduces to  $\sim 40 \text{ kpc}^3$ . The average volume per black hole then becomes  $40\text{-}400 \text{ pc}^3$ , and the expected distance to the nearest black hole drops to  $1.7\text{-}3.6 \text{ pc}$  (5.5-12 ly).

Applying a similar correction to the approach of [Murchikova & Sahu \(2025\)](#), we assume a stellar mass in the spiral arms of  $M_{\text{star}} \sim 1.5 \cdot 10^{10} M_{\odot}$  and negligible black holes elsewhere. Then  $V_{\text{BH}}$  ranges from  $400 \text{ pc}^3$  to  $4,000 \text{ pc}^3$ , implying the nearest black hole lies within  $4.6\text{-}9.8 \text{ pc}$ , with an expected distance of  $3.7\text{-}7.8 \text{ pc}$  (12-25 ly). Thus, if black holes are concentrated in spiral arms, the nearest one could be as close as  $\sim 6\text{-}12 \text{ ly}$  (per [Fender et al. 2013](#)) or  $\sim 12\text{-}25 \text{ ly}$  (per [Murchikova & Sahu 2025](#)). While this scenario likely overestimates the local black hole density, it suggests that the true density may be higher than inferred from a smooth Galactic model.

### 3. SPECTRA OF NEARBY BLACK HOLES ACCRETING FROM THE INTERSTELLAR MEDIUM

Any isolated black hole in the Galaxy is surrounded by the interstellar medium, enabling accretion that may produce detectable electromagnetic radiation ([Shvartsman 1971; Meszaros 1975; McDowell 1985; Fujita et al. 1998; Maccarone 2005; Fender et al. 2013; Tsuna et al. 2018; Scarcella et al. 2021; Murchikova & Sahu 2025](#)).

#### 3.1. Mass Accretion Rate

The standard framework for describing accretion from the interstellar medium onto an isolated compact object is the Bondi-Hoyle-Lyttleton (BHL) model ([Hoyle & Lyttleton 1939; Bondi & Hoyle 1944](#)). In this model, the accretion rate for a black hole of mass  $M_{\text{BH}}$  moving at velocity  $v_{\text{BH}}$  relative to the interstellar medium is

$$\dot{M}_{\text{BHL}} = \frac{4\pi G_{\text{N}}^2 M_{\text{BH}}^2 \rho}{(v_{\text{BH}}^2 + c_s^2)^{3/2}}, \quad (1)$$

where  $G_{\text{N}}$  is Newton's gravitational constant,  $c_s$  is the sound speed in the interstellar medium, and  $\rho$  is the in-

terstellar medium density. The density can be expressed as  $\rho = \mu n m_p$ , where  $\mu$  is the mean atomic mass,  $n$  is the particle number density, and  $m_p$  is the proton mass. To account for outflows and convection, a dimensionless suppression factor  $\lambda < 1$  is often introduced, giving the effective accretion rate as

$$\dot{M}_{\text{BH}} = \lambda \dot{M}_{\text{BHL}}. \quad (2)$$

Numerical simulations typically suggest  $\lambda \approx 0.2\text{-}0.5$  (see, e.g., [Kaaz et al. 2023; Galishnikova et al. 2025](#)).

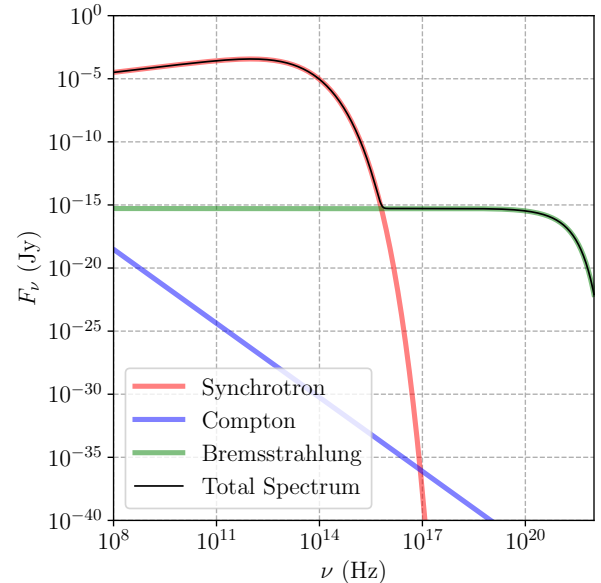


**Figure 1.** Spectrum of an isolated black hole accreting from the interstellar medium as computed with the LLAGNSED model. We assume that the mass accretion rate is described by the BHL model with  $\lambda = 1$  and we employ the following values for the parameters of the system: black hole mass  $M_{\text{BH}} = 10 M_{\odot}$ , black hole distance  $D = 15 \text{ pc}$ , black hole speed  $v_{\text{BH}} = 50 \text{ km s}^{-1}$ , sound speed in the interstellar medium  $c_s = 10 \text{ km s}^{-1}$ , particle number density  $n = 0.3 \text{ cm}^{-3}$ , and mean atomic mass  $\mu = 0.75$ . The resulting Eddington-scaled accretion luminosity is  $\sim 10^{-9}$ . The plot shows the three components of the spectrum: synchrotron radiation, inverse Compton scattering, and bremsstrahlung emission.

An alternative, more advanced framework is the Park-Ricotti (PR) model ([Park & Ricotti 2013](#)), which combines the BHL approach with results from hydrodynamical simulations. In the PR model, the accretion rate is

$$\dot{M}_{\text{PR}} = \frac{4\pi G_{\text{N}}^2 M_{\text{BH}}^2 \rho_{\text{ion}}}{(v_{\text{ion}}^2 + c_{\text{ion}}^2)^{3/2}}, \quad (3)$$

where  $\rho_{\text{ion}}$ ,  $v_{\text{ion}}$ , and  $c_{\text{ion}}$  are the density, relative velocity, and sound speed in the ionized medium surrounding

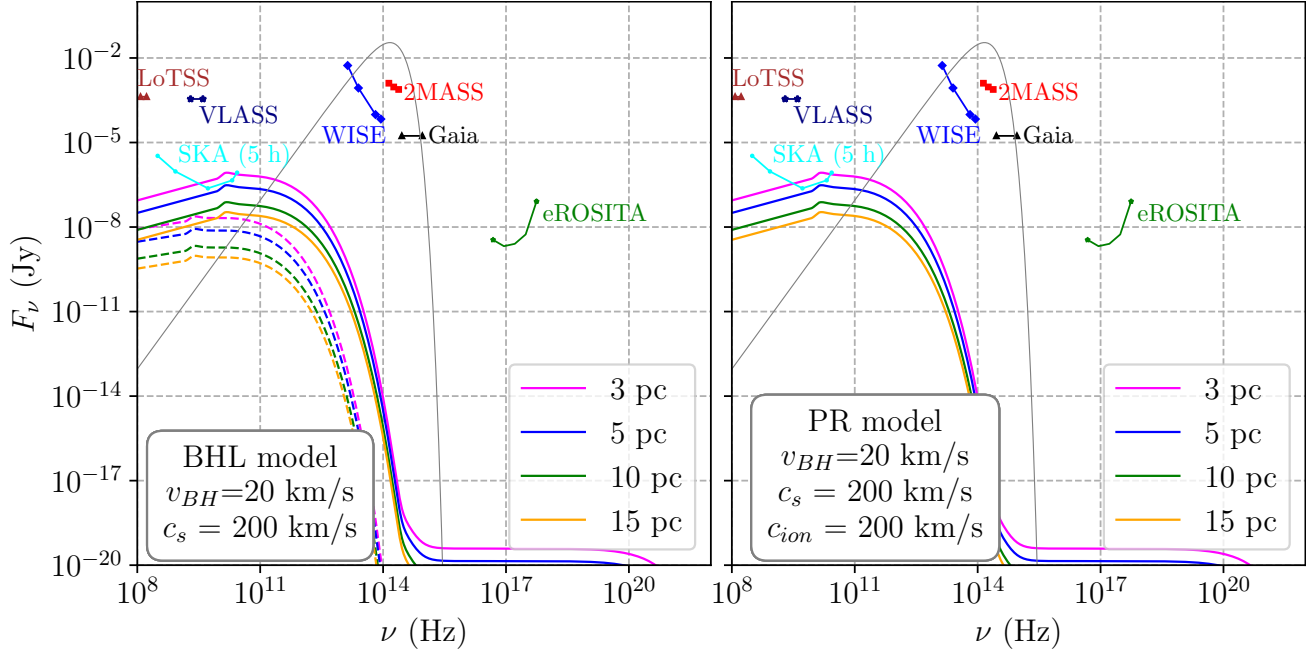


**Figure 2.** Spectra of isolated black holes accreting from a hot and low-density interstellar medium at 3, 5, 10, and 15 pc from the Solar System as computed with `LLAGNSED` (ADAF model). We assume that the particle number density is  $n = 0.05 \text{ cm}^{-3}$ , the mean atomic mass is  $\mu = 0.5$ , the sound speed is  $c_s = 200 \text{ km s}^{-1}$ , the black hole mass is  $M_{\text{BH}} = 10 M_{\odot}$ , and the black hole velocity is  $v_{\text{BH}} = 20 \text{ km s}^{-1}$ . In the left panel, we assume the BHL accretion model with  $\lambda = 1$  (solid) and  $\lambda = 0.1$  (dashed). In the right panel, we assume the PR accretion model with  $c_{\text{ion}} = 200 \text{ km s}^{-1}$ . The gray curve is the spectrum of a brown dwarf with surface temperature  $T = 2,500 \text{ K}$ , radius  $R = 60,000 \text{ km}$ , at a distance of 10 pc, approximated with a blackbody spectrum. We also report the detection thresholds of Gaia DR3 (black), eROSITA (green), 2MASS (red), WISE (blue), VLASS (dark blue), LoTSS (brown), and a 5 hour observation with SKA (cyan).

the black hole, all related to the corresponding interstellar medium quantities as described in Park & Ricotti (2013). The PR model recovers the BHL rate at high  $v_{\text{BH}}$ , predicts higher accretion at intermediate velocities, and predicts significantly lower accretion at low velocities (see quantitative details in Scarella et al. 2021). Unlike the BHL model, the PR formulation does not require an additional suppression factor  $\lambda$ , as such effects are already incorporated.

Within the spherical volume of radius 15 pc around the Solar System ( $\sim 14,000 \text{ pc}^3$ ), 80–95% of the volume is filled with a hot, low-density interstellar medium. The remaining 5–20% is occupied by a complex of warm, partially ionized clouds known as the Cluster of Local Interstellar Clouds (Redfield & Linsky 2008). Other interstellar medium phases are negligible in volume and thus unlikely to host an isolated black hole. In the hot, low-density phase, the particle density is  $n \sim 0.005\text{--}0.05 \text{ cm}^{-3}$ , the mean atomic mass is  $\mu \approx 0.5$ , and the sound speed is  $c_s \sim 200 \text{ km s}^{-1}$  (so  $c_s^2 \gg v_{\text{BH}}^2$ , dominating the accretion rate). In the warm, partially ionized clouds,  $n \sim 0.3 \text{ cm}^{-3}$ ,  $\mu \approx 0.75$ , and  $c_s \sim 10 \text{ km s}^{-1}$  (so

$c_s^2 \ll v_{\text{BH}}^2$ , making  $v_{\text{BH}}$  the main determinant of accretion).

### 3.2. ADAF Model

The accretion rate onto an isolated black hole accreting from the interstellar medium is extremely low. For the BHL model with  $\lambda = 1$ , the Eddington-scaled luminosity of a black hole inside one of the Local Interstellar Clouds is  $\sim 10^{-9}$ . Outside these clouds, in the hot, low-density interstellar medium, this value drops below  $10^{-17}$ . The standard framework for accretion at such low rates is the advection-dominated accretion flow (ADAF) model (Narayan & Yi 1994, 1995a,b).

Following Murchikova & Sahu (2025), we use the public code `LLAGNSED` (Pesce et al. 2021), developed for low-luminosity active galactic nuclei but scalable to stellar-mass black holes. We adopt default parameters and set the black hole mass to  $10 M_{\odot}$ , noting that the model can become unstable for certain input combinations. Fig. 1 shows a representative spectrum from `LLAGNSED`, which combines synchrotron radiation, bremsstrahlung emission, and inverse Compton scattering.

Fig. 2 shows spectra for black holes accreting from the hot, low-density interstellar medium at distances of 3, 5,

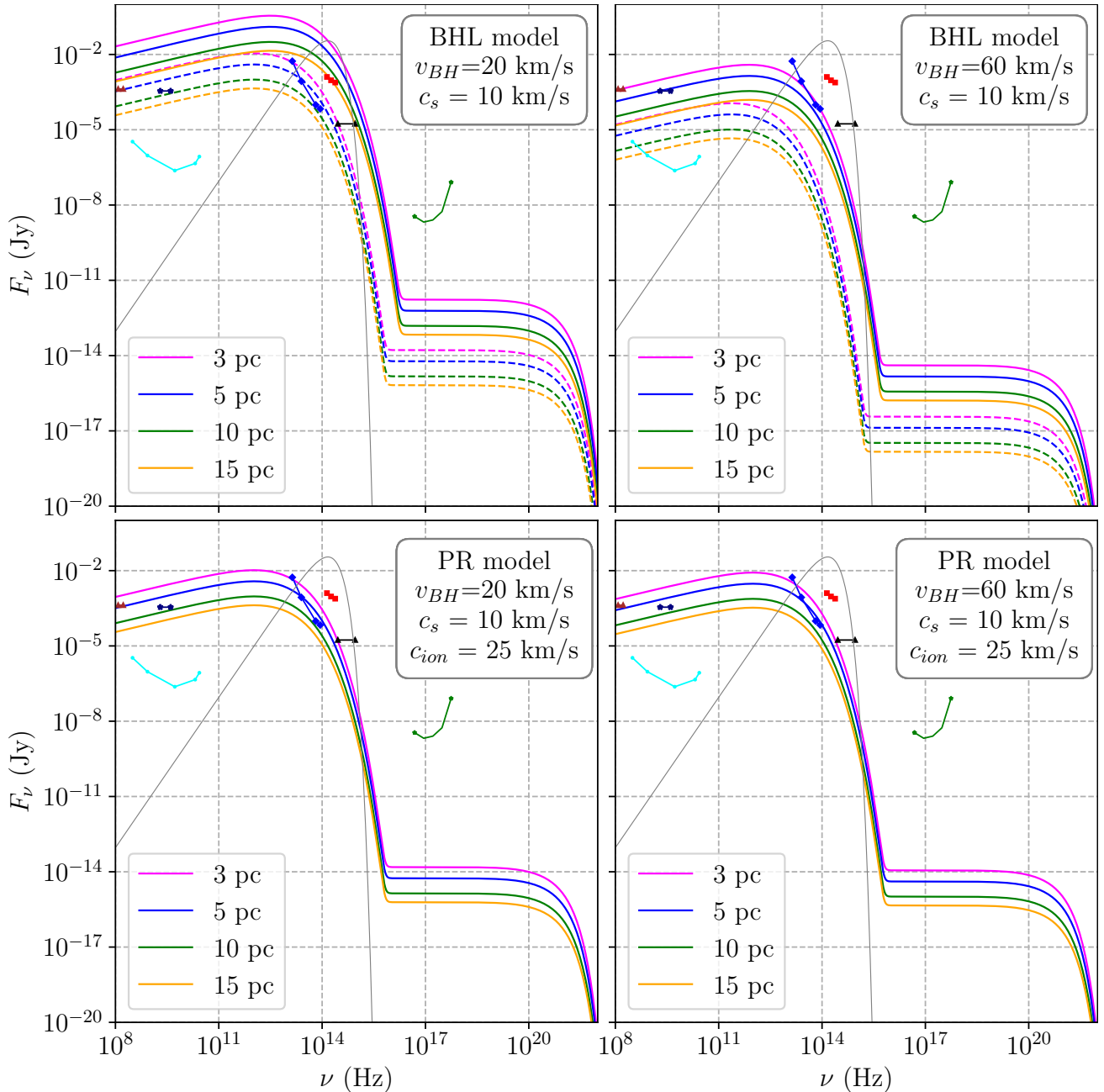


**Figure 3.** Spectra of isolated black holes accreting from a warm and partially ionized interstellar medium at 3, 5, 10, and 15 pc from the Solar System as computed with LLAGNSED (ADAF model). We assume that the particle number density is  $n = 0.3 \text{ cm}^{-3}$ , the mean atomic mass is  $\mu = 0.75$ , the sound speed is  $c_s = 10 \text{ km s}^{-1}$ , and the black hole mass is  $M_{\text{BH}} = 10 M_{\odot}$ . In the top panels, we assume the BHL accretion model with  $\lambda = 1$  (solid) and  $\lambda = 0.1$  (dashed). In the bottom panels, we assume the PR accretion model with  $c_{\text{ion}} = 25 \text{ km s}^{-1}$ . The black hole velocity is  $v_{\text{BH}} = 20 \text{ km s}^{-1}$  in the left panels and  $v_{\text{BH}} = 60 \text{ km s}^{-1}$  in the right panels. The gray curve is the spectrum of a brown dwarf with surface temperature  $T = 2,500 \text{ K}$ , radius  $R = 60,000 \text{ km}$ , at a distance of 10 pc, approximated with a blackbody spectrum. The detection thresholds are the same as in Fig. 2.

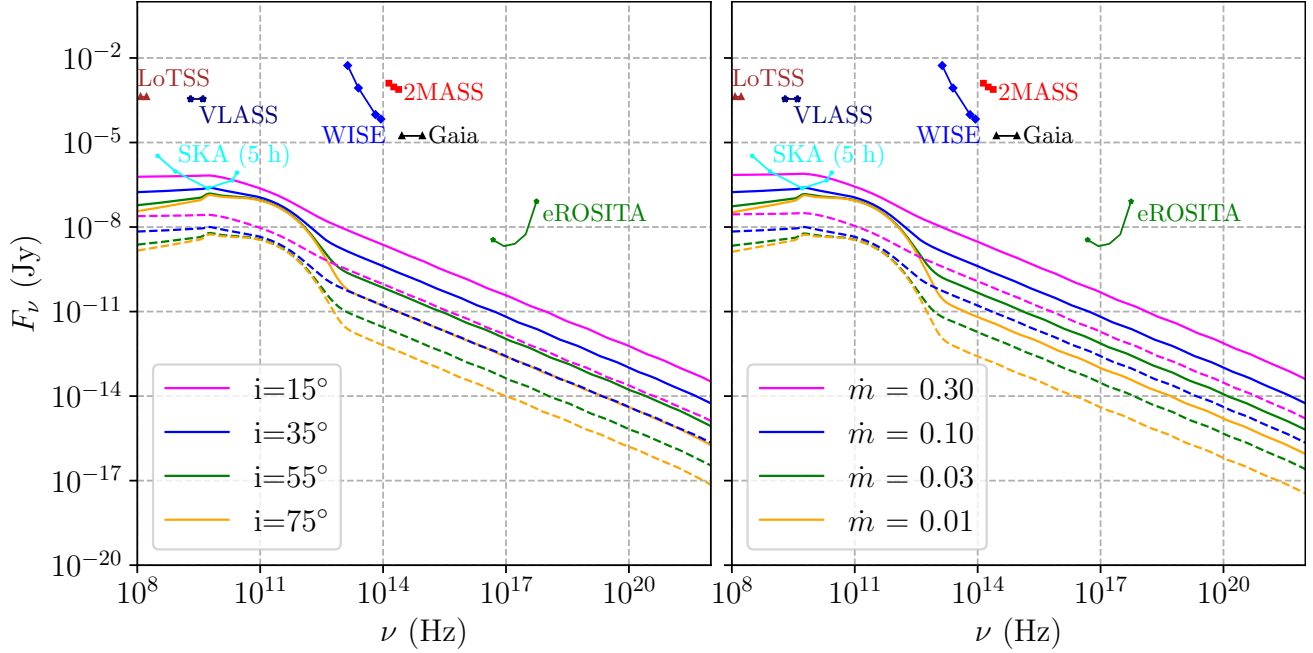


**Figure 4.** Spectra of isolated black holes accreting from a hot and low-density interstellar medium in the ADAF+Jet model. In the left panel, we vary the angle between the jet axis and our line of sight assuming that the mass-loss rate into jet is 10% of the black hole mass accretion rate. In the right panel, we vary the mass-loss rate into jet assuming that the angle between the jet axis and our line of sight is  $35^\circ$ . In both panels, we assume the BHL accretion model with  $\lambda = 0.3$  and we employ the following values for the parameters of the system: particle number density  $n = 0.05 \text{ cm}^{-3}$ , mean atomic mass  $\mu = 0.5$ , sound speed  $c_s = 200 \text{ km s}^{-1}$ , black hole mass  $M_{\text{BH}} = 10 M_{\odot}$ , and black hole velocity  $v_{\text{BH}} = 20 \text{ km s}^{-1}$ . Solid curves are for a black hole distance  $D = 3 \text{ pc}$  and dashed curves are for a black hole distance  $D = 15 \text{ pc}$ . The detection thresholds are the same as in Fig. 2.

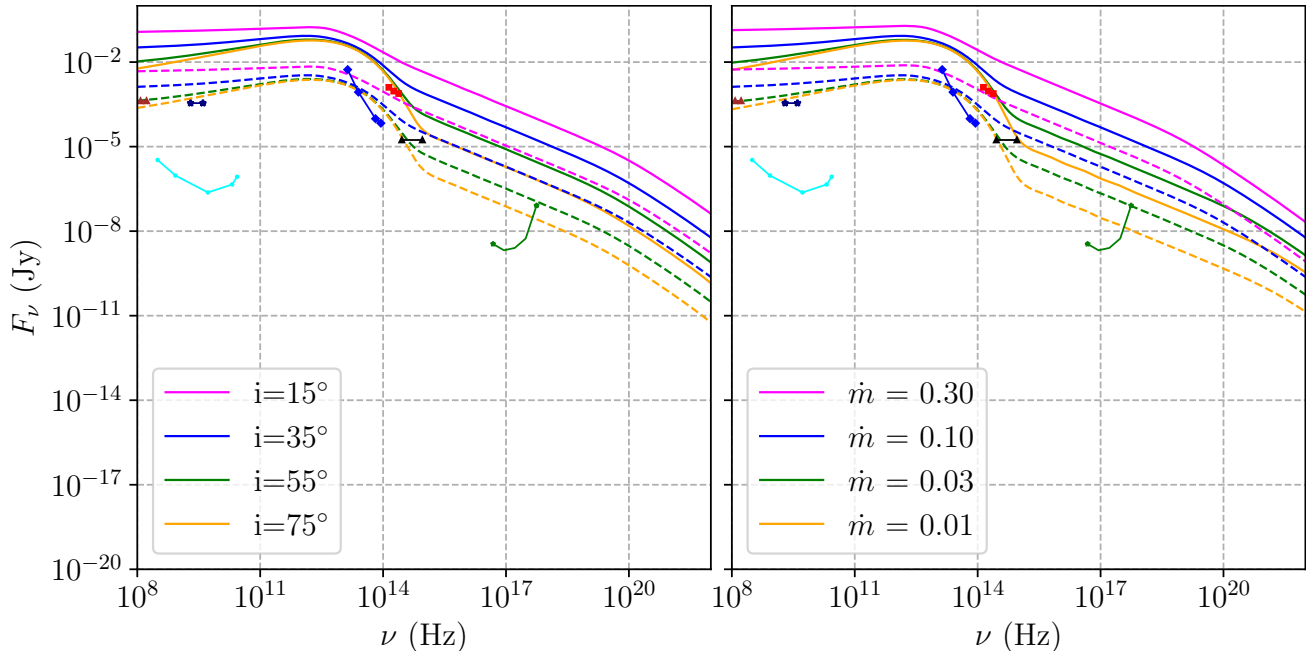


**Figure 5.** Spectra of isolated black holes accreting from a warm and partially ionized interstellar medium in the ADAF+Jet model. In the left panel, we vary the angle between the jet axis and our line of sight assuming that the mass-loss rate into jet is 10% of the black hole mass accretion rate. In the right panel, we vary the mass-loss rate into jet assuming that the angle between the jet axis and our line of sight is  $35^\circ$ . In both panels, we assume the BHL accretion model with  $\lambda = 0.3$  and we employ the following values for the parameters of the system: particle number density  $n = 0.3 \text{ cm}^{-3}$ , mean atomic mass  $\mu = 0.75$ , sound speed  $c_s = 10 \text{ km s}^{-1}$ , black hole mass  $M_{\text{BH}} = 10 M_{\odot}$ , and black hole velocity  $v_{\text{BH}} = 20 \text{ km s}^{-1}$ . Solid curves are for a black hole distance  $D = 3 \text{ pc}$  and dashed curves are for a black hole distance  $D = 15 \text{ pc}$ . The detection thresholds are the same as in Fig. 2.

10, and 15 pc, computed with **LLAGNSED**. The left panel assumes the BHL model; the right panel assumes the PR model. Even for the highest plausible density in this phase ( $n = 0.05 \text{ cm}^{-3}$ ), all predicted spectra lie well below the detection thresholds of current catalogs. Fig. 2 includes sensitivity limits for Gaia DR3 (Gaia Collaboration et al. 2023), eROSITA DR1 (Merloni et al. 2024), 2MASS (Cutri et al. 2003), WISE (Cutri et al. 2013), VLA Sky Survey (VLASS, Lacy et al. 2020), LOFAR Two-metre Sky Survey DR2 (LoTSS DR2, Shimwell et al. 2022), and a 5-hour observation with the Square Kilometre Array (SKA, Braun et al. 2019).

Fig. 3 shows spectra for black holes accreting from the warm, partially ionized clouds. The top panels show BHL predictions for  $\lambda = 1$  (solid) and  $\lambda = 0.1$  (dashed); the bottom panels show PR predictions. Left and right panels assume  $v_{\text{BH}} = 20$  and  $60 \text{ km s}^{-1}$ , respectively. The same sensitivity limits as in Fig. 2 are shown.

In the BHL model, the accretion rate decreases monotonically with  $v_{\text{BH}}$ . Fig. 3 indicates that a black hole in one of the Local Interstellar Clouds may be above current detection thresholds for  $v_{\text{BH}} = 20 \text{ km s}^{-1}$  but fall below them for  $v_{\text{BH}} = 60 \text{ km s}^{-1}$ . In the PR model, the accretion rate peaks around  $v_{\text{BH}} \approx 50 \text{ km s}^{-1}$  for this interstellar medium phase and declines at lower and higher velocities. We caution that the **LLAGNSED** spectra, based on self-similar ADAF solutions with an ad hoc inner cutoff at  $6 r_g$  (where  $r_g = G_N M_{\text{BH}}/c^2$ ), provide a general guide rather than a precise prediction. Altering this inner radius, for example, shifts the synchrotron cutoff to higher energies, which would affect the relative sensitivity of facilities like Gaia and WISE.

### 3.3. ADAF+Jet Model

Evidence suggests that black holes accreting at very low rates may be jet-dominated (Xie et al. 2014; Yang 2016). We therefore combine the ADAF spectrum from **LLAGNSED** with a jet spectrum using the phenomenological model of Xie et al. (2014). We assume a mildly relativistic jet with Lorentz factor 1.8, as suggested by the case of quiescent black hole X-ray binaries. The key-model parameters are the mass-loss rate into the jet,  $\dot{M}_{\text{jet}}$ , and the inclination angle  $i$  between the jet axis and our line of sight. The jet mass-loss rate is constrained by  $\dot{m} \equiv \dot{M}_{\text{jet}}/\dot{M}_{\text{BH}} < 1$ . Details on the model and its parameters can be found in Yuan et al. (2005) and Xie et al. (2016).

Figs. 4 and 5 show the resulting ADAF+Jet spectra for accretion from the hot, low-density interstellar medium and the warm, partially ionized clouds, respectively. In each figure, spectra are shown for black holes at 3 pc and 15 pc, varying either  $\dot{m}$  or  $i$ . Black holes

in the hot interstellar medium remain undetectable even with a jet. For black holes in the warm clouds, however, the jet can significantly enhance detectability, particularly in the radio and X-ray bands. While the eROSITA detection threshold was far above the predicted X-ray emission in the pure ADAF case, the jet component makes the X-ray band a promising avenue for discovery.

We again emphasize that the jet model of Xie et al. (2014) is phenomenological, and its predictions may differ substantially from other jet models. The spectra presented in Figs. 2–5 serve as illustrative examples, but their resemblance to real accretion spectra remains unknown, as no black hole accreting from the interstellar medium has yet been identified.

## 4. SEARCHING FOR NEARBY BLACK HOLES IN GAIA DR3

### 4.1. Accreting Black Holes

Although significant uncertainties remain regarding the local black hole population, the volume fraction occupied by Local Interstellar Clouds, and the precise electromagnetic spectrum of an isolated black hole accreting from the interstellar medium, the discussion in the preceding sections motivates a search for candidate accreting black holes in the Gaia DR3 catalog.

We begin by selecting all Gaia DR3 sources within 15 pc of the Solar System, yielding 1,071 objects<sup>7</sup>. We cross-match these sources with the SIMBAD database<sup>8</sup> to identify known objects and assess their classifications. Of these, five sources have no entry in SIMBAD, and one source is listed as a brown dwarf candidate; the remaining sources are well-classified in SIMBAD. Table 1 presents the source IDs and basic properties for the five SIMBAD-absent sources and the brown dwarf candidate. We note that these six sources do not appear in the unWISE catalog (Schlafly et al. 2019), in 2MASS (Cutri et al. 2003), in the “living” catalog of nearby faint objects Best et al. (2025), and in the list of new nearby sources in Vrba et al. (2026).

These six faint sources (all near the Gaia detection limit) are potential candidates for isolated black holes accreting from the interstellar medium. However, the brown dwarf candidate can be excluded as a stellar-mass black hole, as it resides in a binary system (Scholz 2021).

<sup>7</sup> We note that the assumption that distance is the inverse of parallax is only valid for high signal-to-noise ratio values of the parallax but can give highly biased results in general (Bailer-Jones et al. 2021). In our case, the high signal-to-noise ratio condition is met.

<sup>8</sup> <https://simbad.u-strasbg.fr/simbad/>

**Table 1.** Sources within 15 pc of the Solar System in the Gaia DR3 catalog and without a clear classification. The precision of the position in the sky of these sources is at the level of 1-2 mas in the Gaia DR3 and is not reported in this table, where we truncate the Galactic coordinates at the second decimal digit. The G magnitude of source 4114677389434590720 is not available in `gaia_source` but at <https://www.cosmos.esa.int/web/gaia/dr3-known-issues#PhotometryMissingGFluxes>.

Source ID	Galactic Coordinates	Parallax	G Magnitude	Classification
2021981409373336448	(61.57°, 1.73°)	76.2 ± 2.8	20.7	Unknown Source
3489874340630661248	(292.04°, 38.33°)	94.2 ± 1.1	20.6	Brown Dwarf Candidate
4039831777499368960	(352.65°, -4.79°)	81.8 ± 2.9	20.0	Unknown Source
4114677389434590720	(1.84°, 8.40°)	67.9 ± 2.7	20.4	Unknown Source
4269379774976572160	(38.61°, -1.67°)	84.4 ± 2.5	20.0	Unknown Source
4318384355378007424	(51.87°, -2.47°)	101 ± 3	20.6	Unknown Source

The five sources not in SIMBAD all lie near the Galactic plane. While no further information is available from the public Gaia DR3 catalog, their locations make it likely that they are spurious astrometric solutions: the Galactic plane is a region of crowding which is challenging for Gaia. Such sources may be removed in Gaia DR4, scheduled for release in December 2026.

We note that Gaia DR3 contains sources without parallax measurements<sup>9</sup>. Many are faint and could be of interest, but their distances cannot be determined from the public catalog. Parallaxes for some may become available in Gaia DR4.

#### 4.2. Non-Accreting Black Holes

Indirect detection of an isolated black hole within 15 pc through its gravitational influence on nearby stars is highly unlikely due to the low local stellar density.

The stellar velocity dispersion in the Solar neighborhood is  $\sigma \sim 20 \text{ km s}^{-1}$ . A close encounter between a star and a black hole could produce a high-velocity star. The radius of influence of the black hole is approximately  $R \sim 2G_N M_{\text{BH}}/\sigma^2 \sim 0.2 \text{ mpc}$ . With  $\sim 10^3$  stars within 15 pc (stellar density  $n_{\text{stars}} \sim 0.08 \text{ pc}^{-3}$ ), the probability of such an encounter per black hole per year is

$$\Gamma \sim n_{\text{stars}} \sigma \pi R^2 \sim 2 \times 10^{-13} \text{ yr}^{-1} \text{ BH}^{-1}.$$

Assuming 10 black holes within this volume, the total encounter rate is  $\sim 10^{-12} \text{ yr}^{-1}$ , which is far too low for a detectable event within any plausible observational timescale.

<sup>9</sup> Gaia DR3 includes sources with two (position only), five (position, parallax, proper motion), or six (adding source color) astrometric parameters. Sources with insufficient observations or poor astrometric fits lack a measured parallax.

#### 5. CONCLUDING REMARKS

It is plausible that one or more stellar-mass black holes reside within 15 pc of the Solar System. Most stellar-mass black holes are expected to be isolated, and the majority of those in binary systems likely have another black hole as a companion. This makes their direct detection particularly challenging.

If such a black hole is located within one of the Local Interstellar Clouds – which collectively occupy 5-20% of the local volume – accretion from the interstellar medium could produce a detectable electromagnetic signal. However, substantial uncertainties in the expected accretion spectra complicate the formulation of a definitive observational strategy. For a simple advection-dominated accretion flow (ADAF) spectrum, detection may be more feasible in the radio to optical bands. If the spectrum is jet-dominated, wide-area X-ray surveys could prove more effective for identifying these faint sources. Conversely, black holes outside these clouds, surrounded by the hot, low-density interstellar medium, have accretion luminosities too low for detection with current or near-future facilities, regardless of the accretion model.

Motivated by the possibility of a black hole within one of the Local Interstellar Clouds, we searched the Gaia DR3 catalog for candidate objects. Of the 1,071 sources within 15 pc with measured parallaxes, only six lack a clear classification: five are absent from SIMBAD, and one is listed as a brown dwarf candidate. The latter can be excluded as a stellar-mass black hole because it resides in a binary system. The five SIMBAD-absent sources all lie near the Galactic plane, making them likely spurious astrometric solutions, for instance caused by unmodelled background sources (crowding) and/or unmodelled binarity, though their nature can-

not be definitively ascertained from the public catalog alone.

Constructing a physically motivated list of expected Gaia properties to aid candidate selection is unfortunately not feasible. As noted by [Murchikova & Sahu \(2025\)](#), an isolated black hole accreting from the interstellar medium would appear as a faint source with a relatively featureless spectrum. Consequently, identification cannot rely on single-instrument observations. Multi-wavelength follow-up campaigns, covering radio, optical, and X-ray bands, are necessary to rule out alternative interpretations and confirm the nature of any candidate.

Future efforts will focus on searching for isolated black holes accreting from the warm, partially ionized interstellar medium in radio and X-ray catalogs. The forthcoming release of Square Kilometre Array (SKA) data,

currently anticipated in the first half of 2027, appears especially promising for this endeavor.

**Acknowledgments** – This work was supported by the National Natural Science Foundation of China (NSFC), Grant No. W2531002, and the Fudan-Warwick Joint Seed Fund, Grant No. JMH6282518. A.N. also acknowledges the support from the Shanghai Government Scholarship (SGS). F.G.X. is supported in part by the National Natural Science Foundation of China (NSFC), Grant No. 12373017, and the State Key Laboratory of Radio Astronomy and Technology (Chinese Academy of Sciences). This work has made use of data from the European Space Agency (ESA) mission *Gaia* (<https://www.cosmos.esa.int/gaia>), processed by the *Gaia* Data Processing and Analysis Consortium (DPAC, <https://www.cosmos.esa.int/web/gaia/dpac/consortium>). Funding for the DPAC has been provided by national institutions, in particular the institutions participating in the *Gaia* Multilateral Agreement.

## REFERENCES

Abbott, B. P., Abbott, R., Abbott, T. D., et al. 2016, *PhRvL*, 116, 221101, doi: [10.1103/PhysRevLett.116.221101](https://doi.org/10.1103/PhysRevLett.116.221101)

—. 2019, *PhRvD*, 100, 104036, doi: [10.1103/PhysRevD.100.104036](https://doi.org/10.1103/PhysRevD.100.104036)

Abdulghani, Y., Lohfink, A. M., & Chauhan, J. 2025, *MNRAS*, 541, 553, doi: [10.1093/mnras/staf979](https://doi.org/10.1093/mnras/staf979)

Bailer-Jones, C. A. L., Rybizki, J., Fouesneau, M., Demleitner, M., & Andrae, R. 2021, *AJ*, 161, 147, doi: [10.3847/1538-3881/abd806](https://doi.org/10.3847/1538-3881/abd806)

Bambi, C. 2017a, *Reviews of Modern Physics*, 89, 025001, doi: [10.1103/RevModPhys.89.025001](https://doi.org/10.1103/RevModPhys.89.025001)

—. 2017b, *Black Holes: A Laboratory for Testing Strong Gravity* (Springer Singapore), doi: [10.1007/978-981-10-4524-0](https://doi.org/10.1007/978-981-10-4524-0)

—. 2025a, *iScience*, 28, 113142, doi: [10.1016/j.isci.2025.113142](https://doi.org/10.1016/j.isci.2025.113142)

—. 2025b, *arXiv* e-prints, arXiv:2509.11222, doi: [10.48550/arXiv.2509.11222](https://doi.org/10.48550/arXiv.2509.11222)

Bambi, C., & Cárdenas-Avendaño, A. 2024, *Recent Progress on Gravity Tests. Challenges and Future Perspectives* (Springer Singapore), doi: [10.1007/978-981-97-2871-8](https://doi.org/10.1007/978-981-97-2871-8)

Best, W. M. J., Dupuy, T. J., Liu, M. C., et al. 2025, *The UltracoolSheet: Photometry, Astrometry, Spectroscopy, and Multiplicity for 4000+ Ultracool Dwarfs and Imaged Exoplanets*, 2.1.0, Zenodo, doi: [10.5281/zenodo.15802304](https://doi.org/10.5281/zenodo.15802304)

Bondi, H., & Hoyle, F. 1944, *MNRAS*, 104, 273, doi: [10.1093/mnras/104.5.273](https://doi.org/10.1093/mnras/104.5.273)

Braun, R., Bonaldi, A., Bourke, T., Keane, E., & Wagg, J. 2019, *arXiv* e-prints, arXiv:1912.12699, doi: [10.48550/arXiv.1912.12699](https://doi.org/10.48550/arXiv.1912.12699)

Cao, Z., Nampalliwar, S., Bambi, C., Dauser, T., & García, J. A. 2018, *PhRvL*, 120, 051101, doi: [10.1103/PhysRevLett.120.051101](https://doi.org/10.1103/PhysRevLett.120.051101)

Carter, B. 1971, *PhRvL*, 26, 331, doi: [10.1103/PhysRevLett.26.331](https://doi.org/10.1103/PhysRevLett.26.331)

Cutri, R. M., Skrutskie, M. F., van Dyk, S., et al. 2003, *2MASS All Sky Catalog of point sources*.

Cutri, R. M., Wright, E. L., Conrow, T., et al. 2013, *Explanatory Supplement to the AllWISE Data Release Products*, *Explanatory Supplement to the AllWISE Data Release Products*, by R. M. Cutri et al.

Fender, R. P., Maccarone, T. J., & Heywood, I. 2013, *MNRAS*, 430, 1538, doi: [10.1093/mnras/sts688](https://doi.org/10.1093/mnras/sts688)

Fujita, Y., Inoue, S., Nakamura, T., Manmoto, T., & Nakamura, K. E. 1998, *ApJL*, 495, L85, doi: [10.1086/311220](https://doi.org/10.1086/311220)

Gaia Collaboration, Vallenari, A., Brown, A. G. A., et al. 2023, *A&A*, 674, A1, doi: [10.1051/0004-6361/202243940](https://doi.org/10.1051/0004-6361/202243940)

Galishnikova, A., Philippov, A., Quataert, E., Chatterjee, K., & Liska, M. 2025, *ApJ*, 978, 148, doi: [10.3847/1538-4357/ad9926](https://doi.org/10.3847/1538-4357/ad9926)

Hoyle, F., & Lyttleton, R. A. 1939, Proceedings of the Cambridge Philosophical Society, 35, 405, doi: [10.1017/S0305004100021150](https://doi.org/10.1017/S0305004100021150)

Kaaz, N., Murguia-Berthier, A., Chatterjee, K., Liska, M. T. P., & Tchekhovskoy, A. 2023, ApJ, 950, 31, doi: [10.3847/1538-4357/acc7a1](https://doi.org/10.3847/1538-4357/acc7a1)

Kerr, R. P. 1963, PhRvL, 11, 237, doi: [10.1103/PhysRevLett.11.237](https://doi.org/10.1103/PhysRevLett.11.237)

Lacy, M., Baum, S. A., Chandler, C. J., et al. 2020, PASP, 132, 035001, doi: [10.1088/1538-3873/ab63eb](https://doi.org/10.1088/1538-3873/ab63eb)

Lattimer, J. M. 2012, Annual Review of Nuclear and Particle Science, 62, 485, doi: [10.1146/annurev-nucl-102711-095018](https://doi.org/10.1146/annurev-nucl-102711-095018)

Lutsenko, A., Carraro, G., Korchagin, V., Tkachenko, R., & Vieira, K. 2025, ApJ, 990, 88, doi: [10.3847/1538-4357/ade66](https://doi.org/10.3847/1538-4357/ade66)

Maccarone, T. J. 2005, MNRAS, 360, L30, doi: [10.1111/j.1745-3933.2005.00039.x](https://doi.org/10.1111/j.1745-3933.2005.00039.x)

Maoz, E. 1998, ApJL, 494, L181, doi: [10.1086/311194](https://doi.org/10.1086/311194)

McDowell, J. 1985, MNRAS, 217, 77, doi: [10.1093/mnras/217.1.77](https://doi.org/10.1093/mnras/217.1.77)

Merloni, A., Lamer, G., Liu, T., et al. 2024, A&A, 682, A34, doi: [10.1051/0004-6361/202347165](https://doi.org/10.1051/0004-6361/202347165)

Meszaros, P. 1975, A&A, 44, 59

Murchikova, L., & Sahu, K. C. 2025, ApJL, 988, L12, doi: [10.3847/2041-8213/ade7f8](https://doi.org/10.3847/2041-8213/ade7f8)

Narayan, R., & Yi, I. 1994, ApJL, 428, L13, doi: [10.1086/187381](https://doi.org/10.1086/187381)

—. 1995a, ApJ, 444, 231, doi: [10.1086/175599](https://doi.org/10.1086/175599)

—. 1995b, ApJ, 452, 710, doi: [10.1086/176343](https://doi.org/10.1086/176343)

Olejak, A., Belczynski, K., Bulik, T., & Sobolewska, M. 2020, A&A, 638, A94, doi: [10.1051/0004-6361/201936557](https://doi.org/10.1051/0004-6361/201936557)

Park, K., & Ricotti, M. 2013, ApJ, 767, 163, doi: [10.1088/0004-637X/767/2/163](https://doi.org/10.1088/0004-637X/767/2/163)

Pesce, D. W., Palumbo, D. C. M., Narayan, R., et al. 2021, ApJ, 923, 260, doi: [10.3847/1538-4357/ac2eb5](https://doi.org/10.3847/1538-4357/ac2eb5)

Psaltis, D., Medeiros, L., Christian, P., et al. 2020, PhRvL, 125, 141104, doi: [10.1103/PhysRevLett.125.141104](https://doi.org/10.1103/PhysRevLett.125.141104)

Redfield, S., & Linsky, J. L. 2008, ApJ, 673, 283, doi: [10.1086/524002](https://doi.org/10.1086/524002)

Rhoades, C. E., & Ruffini, R. 1974, PhRvL, 32, 324, doi: [10.1103/PhysRevLett.32.324](https://doi.org/10.1103/PhysRevLett.32.324)

Robinson, D. C. 1975, PhRvL, 34, 905, doi: [10.1103/PhysRevLett.34.905](https://doi.org/10.1103/PhysRevLett.34.905)

Scarella, F., Gaggero, D., Connors, R., et al. 2021, MNRAS, 505, 4036, doi: [10.1093/mnras/stab1533](https://doi.org/10.1093/mnras/stab1533)

Schlafly, E. F., Meisner, A. M., & Green, G. M. 2019, ApJS, 240, 30, doi: [10.3847/1538-4365/aafbea](https://doi.org/10.3847/1538-4365/aafbea)

Scholz, R.-D. 2021, Research Notes of the American Astronomical Society, 5, 40, doi: [10.3847/2515-5172/abea23](https://doi.org/10.3847/2515-5172/abea23)

Shimwell, T. W., Hardcastle, M. J., Tasse, C., et al. 2022, A&A, 659, A1, doi: [10.1051/0004-6361/202142484](https://doi.org/10.1051/0004-6361/202142484)

Shvartsman, V. F. 1971, Soviet Ast., 15, 377

Timmes, F. X., Woosley, S. E., & Weaver, T. A. 1996, ApJ, 457, 834, doi: [10.1086/176778](https://doi.org/10.1086/176778)

Tripathi, A., Nampalliwar, S., Abdikamalov, A. B., et al. 2019a, ApJ, 875, 56, doi: [10.3847/1538-4357/ab0e7e](https://doi.org/10.3847/1538-4357/ab0e7e)

Tripathi, A., Zhang, Y., Abdikamalov, A. B., et al. 2021, ApJ, 913, 79, doi: [10.3847/1538-4357/abf6cd](https://doi.org/10.3847/1538-4357/abf6cd)

Tripathi, A., Yan, J., Yang, Y., et al. 2019b, ApJ, 874, 135, doi: [10.3847/1538-4357/ab0a00](https://doi.org/10.3847/1538-4357/ab0a00)

Tsuna, D., Kawanaka, N., & Totani, T. 2018, MNRAS, 477, 791, doi: [10.1093/mnras/sty699](https://doi.org/10.1093/mnras/sty699)

Vagnozzi, S., Roy, R., Tsai, Y.-D., et al. 2023, Classical and Quantum Gravity, 40, 165007, doi: [10.1088/1361-6382/acd97b](https://doi.org/10.1088/1361-6382/acd97b)

Vrba, F. J., Schneider, A. C., Munn, J. A., et al. 2026, arXiv e-prints, arXiv:2601.09671, doi: [10.48550/arXiv.2601.09671](https://doi.org/10.48550/arXiv.2601.09671)

Xie, F.-G., Yang, Q.-X., & Ma, R. 2014, MNRAS, 442, L110, doi: [10.1093/mnrasl/slu068](https://doi.org/10.1093/mnrasl/slu068)

Xie, F.-G., Zdziarski, A. A., Ma, R., & Yang, Q.-X. 2016, MNRAS, 463, 2287, doi: [10.1093/mnras/stw2132](https://doi.org/10.1093/mnras/stw2132)

Yagi, K., & Stein, L. C. 2016, Classical and Quantum Gravity, 33, 054001, doi: [10.1088/0264-9381/33/5/054001](https://doi.org/10.1088/0264-9381/33/5/054001)

Yang, Q.-X. 2016, Research in Astronomy and Astrophysics, 16, 62, doi: [10.1088/1674-4527/16/4/062](https://doi.org/10.1088/1674-4527/16/4/062)

Yuan, F., Cui, W., & Narayan, R. 2005, ApJ, 620, 905, doi: [10.1086/427206](https://doi.org/10.1086/427206)